Simulation of the cathode surface damages in a HOPFED during ion bombardment

Hongping Zhao, Wei Lei,[a] Xiaobing Zhang, Xiaohua Li, and Qilong Wang
Department of Electronic Engineering, Southeast University, Nanjing 210096, People's Republic of China

(Received 25 July 2005; accepted 13 October 2005; published 7 December 2005)

Most vacuum devices are hampered by ion bombardment due to residual gases. Sometimes, it causes the breakdown of devices and shortens their life. In this article, the effect of the ion bombardment on the cathode surface in a structure of a field emission display was simulated. In this structure, a special type of spacer was used, named "hop" and "flu" spacer. The trajectories of electrons emitted by a cold cathode were calculated under influence of an electric field. From these calculations, the ionization of a residual gas and the corresponding trajectories of the positive ions were estimated. In this article, we modeled Si microtip and Mo microtip field emitters. Because inert gases are not easily absorbed by the getter, several different types of residual gases, such as neon, argon, krypton, and xenon, were introduced in the simulation. The simulation results show that ion bombardment damages on a silicon target induced by Ar, Kr, and Xe are more destructive than Ne. Also, Ar, Kr, and Xe are shown to be more destructive than Ne to a molybdenum microtip. The results obtained in this article suggest damage on Si is larger than that on Mo under the same ion bombardment and that a molybdenum emitter is more stable than a silicon emitter in a nonideal vacuum environment. © *2005 American Vacuum Society.* [DOI: 10.1116/1.2134720]

I. INTRODUCTION

Ion bombardment is an important degradation mechanism for both thermionic and cold cathodes. Electrons emitting from the cathode are accelerated and cause ionization of residual gas atoms in vacuum electronic devices. Positively charged ions are accelerated backwards to the cathode surface under the electric field effect. Then the cathode surface may be damaged by this ion bombardment. The damage on the cathode surface will give rise to current degradation and emission instability and limits the lifetime of vacuum electronic devices. The effect of ion bombardment depends on the electron current emission as well as the pressure and the type of the residual gases. Although a getter in the vacuum device can improve the vacuum condition, the inert gases are practically not be absorbed by the getter. Hence, in order to analyze the degradation of the field emitters, it is important to study ion bombardment induced by inert gases.

To improve the characteristics of a field emission display (FED), LG.Philips Displays proposed a HOPFED structure.[1] In this structure, a special type of spacer named "hop" and "flu" spacer was used. In this article, the damages on a Si microtip and a Mo microtip, caused by the different ionized inert gases, are analyzed.

II. MECHANISM OF THE CATHODE DAMAGE CAUSED BY THE ION BOMBARDMENT IN A HOPFED

A. Simulation model

A HOPFED structure has been proposed for a field emission display.[1] This structure has improved inner-pixel brightness uniformity. Besides this, the field emitters can be protected from the ion bombardment.[2] Figure 1 gives the structure of a HOPFED element. In Fig. 1, the primary electrons emit from cathode, some of which travel through the channel directly, but most of the electrons will impinge on the hop and flu spacers. These electrons are hopping along the insulator surface. Finally, they also reach the screen.[3]

In Fig. 1, the ionization may happen in the hop region as well as in the acceleration region. The primary electrons, the secondary electrons, and the scattered electrons can ionize the residual gas atoms.

B. Secondary electron generation in the hop region

When an electron impinges on a dielectric wall, it may be backscattered (elastically or inelastically) or it may penetrate the dielectric wall.[4,5] When the electron penetrates the dielectric wall, surrounding electrons in the material become heated up (secondary electrons). Some of these secondary electrons may reach the surface and leave the material. Consequently, a "primary" electron impinging on a material generates secondary electrons.

The number of secondary electrons generated per incoming electron (secondary electron yield curve δ) depends on the incoming velocity of the primary electron and on the material properties of the dielectric wall. In Fig. 2 a typical yield curve is plotted.[6–10] There are two characteristics energies $E1$ and $E2$ where the secondary electron yield is equal to 1. These two values are strongly material dependent.

C. Ionization and sputtering model

In Fig. 1, both the primary electrons and the secondary electrons collide with residual gas atoms. During the collision, the neutral atoms of residual gases will be positive

[a]Author to whom correspondence should be addressed; electronic mail: lw@seu.edu.cn

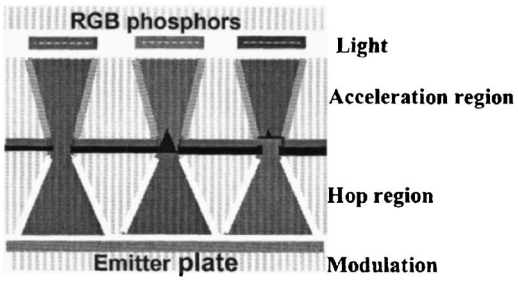

FIG. 1. Structure of HOPFED.

charged. The positive ions are accelerated toward the cathode by the electric field. As shown in Fig. 3, the positive ions bombard the cathode and will damage the cathode surface.[11,12]

The damage of the cathode surface from ion bombardment depends on the composition of surface layer, the cathode material, projectile mass, energy, and ionization. In this article, we used silicon and molybdenum as two types of cathode materials, and used neon, argon, krypton, and xenon as residual gases.

Zalm suggested a semiempirical relation for the sputtering yiels Y in atoms per ion based on the Sigmund model[13]

$$Y = Y_0 S_n(\varepsilon), \tag{1}$$

where Y_0 is a constant depending on the target and projectile type, and S_n represents the so called reduced nuclear or elastic stopping as a function of the reduced energy ε, i.e., the incident projectile energy in the center-off-mass system divided by the Coulomb energy of the target and projectile nuclei at the screening distance

$$\varepsilon = \frac{E_p}{E_0}, \tag{2}$$

where E_p is the projectile's kinetic energy, and E_0 is a normalizing constant according to Sigmund's theory

$$E_0 = \left(1 + \frac{M_p}{M_t}\right) Z_t Z_p (Z_t^{2/3} + Z_p^{2/3})^{1/2} \frac{1}{32.5} \text{keV} \tag{3}$$

with M_p and M_t the projectile's and target's atomic mass, and Z_p and Z_t the respective atomic number. For the reduced

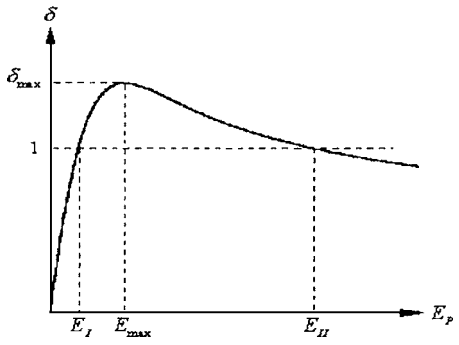

FIG. 2. Secondary electron yield curve δ as a function of the energy of the primary electron.

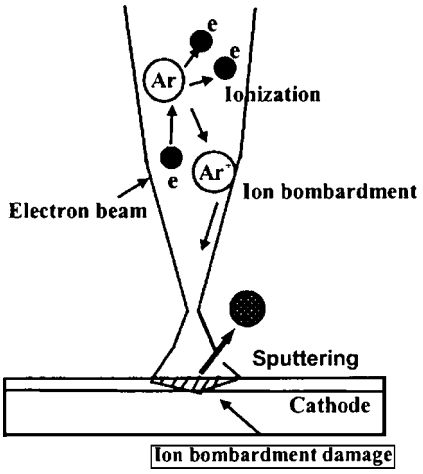

FIG. 3. Conceptual ionization and sputtering model, positive ions are accelerated toward the cathode by the electric field and make damages on the cathode surface.

nuclear or elastic stopping Zalm suggests the use of the approximation by Wilson, Haggmark, and Biersack

$$S_n(\varepsilon) = \frac{\frac{1}{2}\ln(1+\varepsilon)}{\varepsilon + 0.14\varepsilon^{0.42}}. \tag{4}$$

The numerical value of Y_0 can either be fitted to the experimental data or be taken from Sigmunds theory

$$Y_0 = \frac{3.56 \text{ eV}}{U_0} \frac{Z_t Z_p}{(Z_t^{2/3} + Z_p^{2/3})^{1/2}} \frac{M_p}{M_t + M_p} \alpha_s\left(\frac{M_t}{M_p}\right). \tag{5}$$

The average binding energy or escape barrier U_0 is taken to be the sublimation energy for metals (6.8 eV for Mo), or the

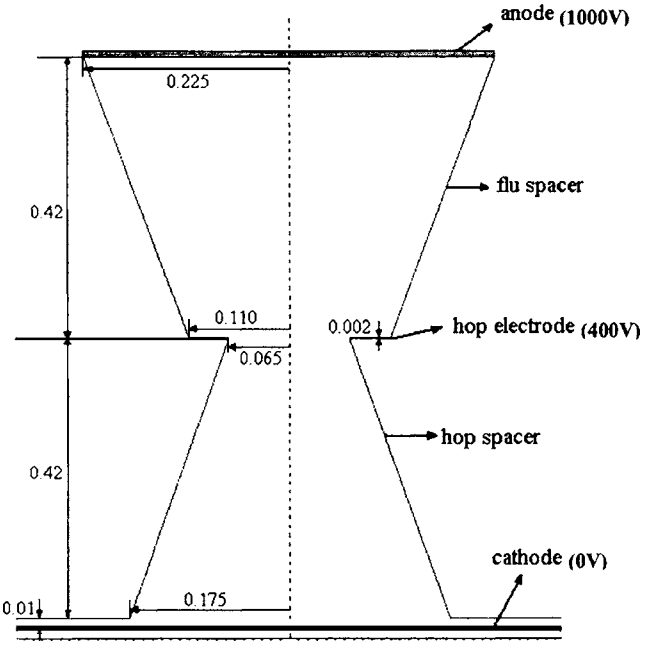

FIG. 4. Two-dimensional model of the simulation structure with hop spacer and flu spacer.

TABLE I. Cathode material and residual gas type calculated in this article.

Simulation	Target	Residual gas type
1	Silicon	Neon
2	Silicon	Argon
3	Silicon	Krypton
4	Silicon	Xenon
5	Molybdenum	Neon
6	Molybdenum	Argon
7	Molybdenum	Krypton
8	Molybdenum	Xenon

cohesive energy for covalent materials (7.8 eV for Si). The dimensionless function α_s depends weakly on energy for $\varepsilon \geqslant 1$ only, and for low to intermediate energies is approximated within 2% by

$$\alpha_s = 0.15 + 0.13\frac{M_t}{M_p}. \tag{6}$$

We used these formulas in our simulation model.

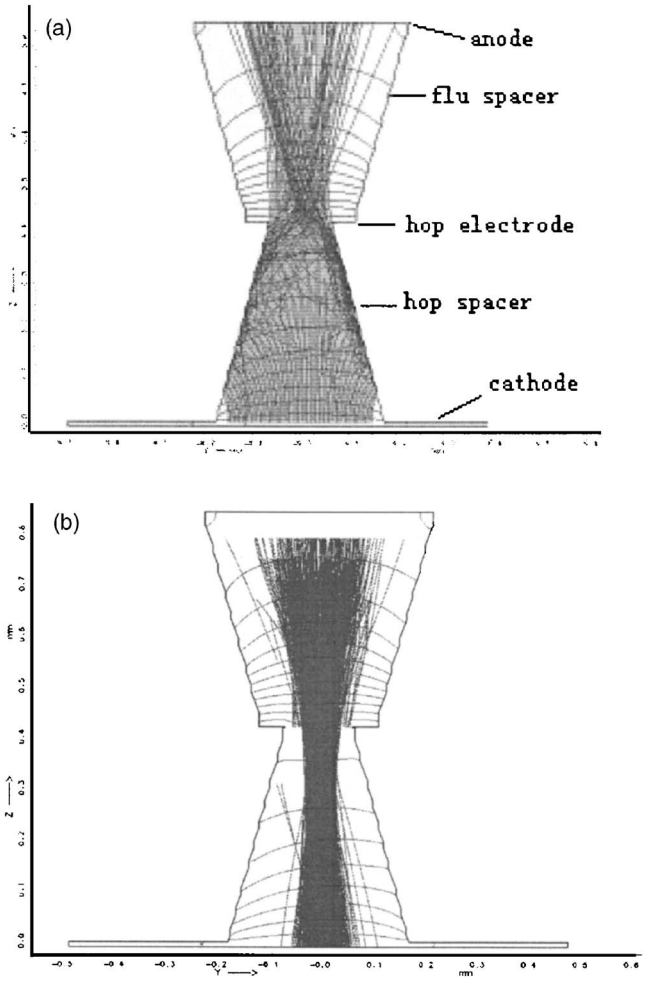

FIG. 5. (a) Potential distribution and electron trajectory when the surface charge on the dielectric wall reach static state. (b) Positive ion trajectories inside the spacer.

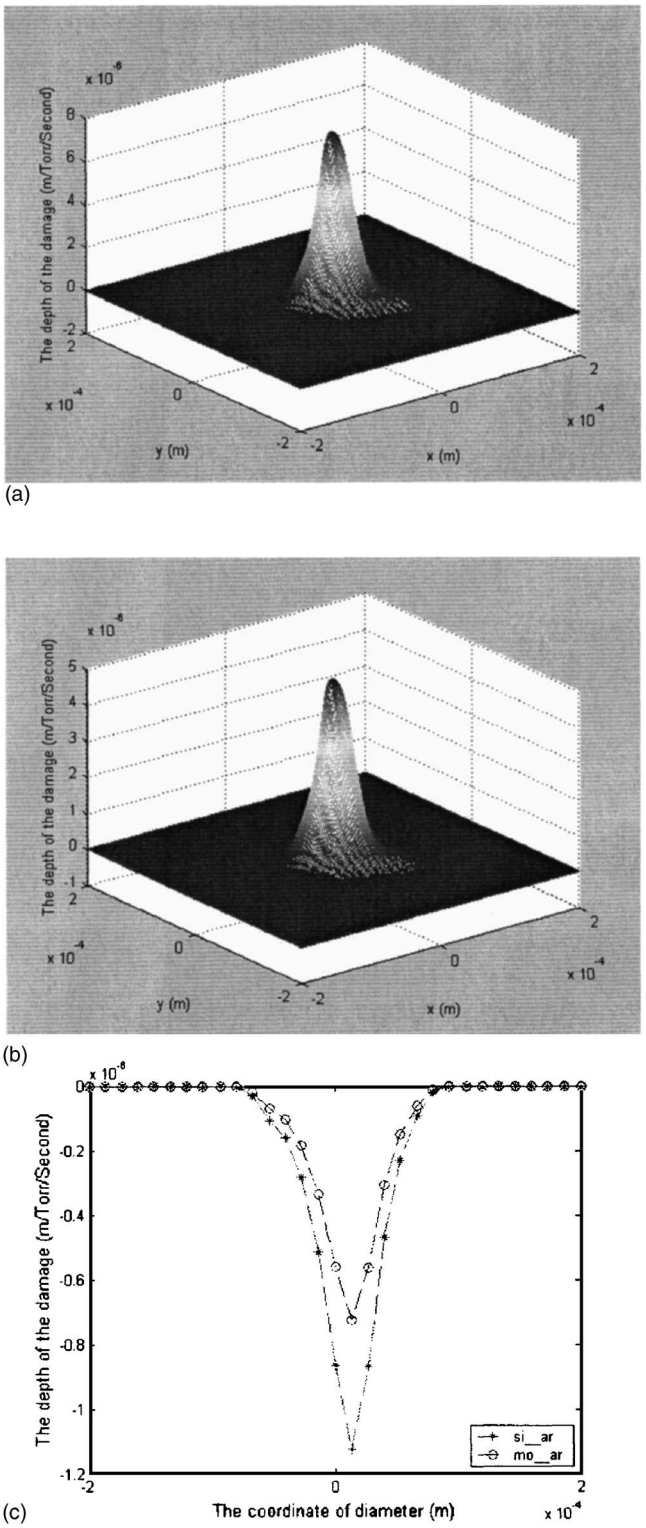

FIG. 6. (a) Ion bombardment damage induced by argon on a Si-microtip cathode. (b) Ion bombardment damage induced by argon on a Mo-microtip cathode. (c) Comparison of the damage induced by argon on a Si-microtip and Mo-microtip cathode.

III. STUDY OF THE CATHODE DAMAGE UNDER DIFFERENT ION BOMBARDMENT CONDITIONS

The HOPFED geometry used in the simulation discussed in this article is shown in Fig. 4. Voltages applied on the

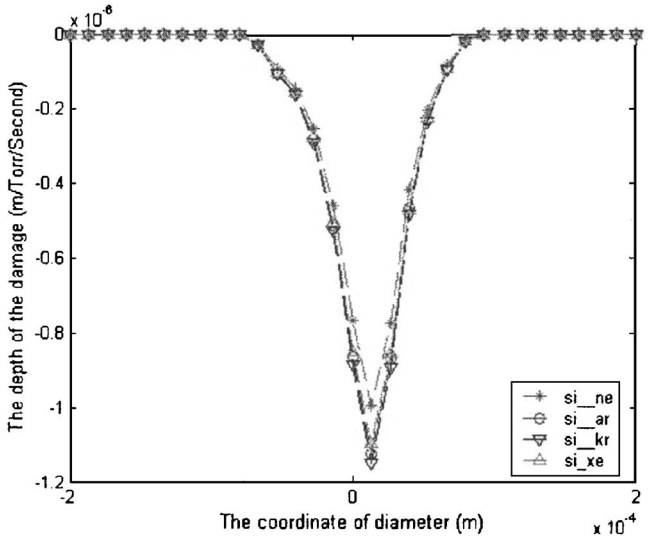

FIG. 7. Comparison of the ion bombardment damages induced by Ne, Ar, Kr, and Xe on a Si-microtip cathode.

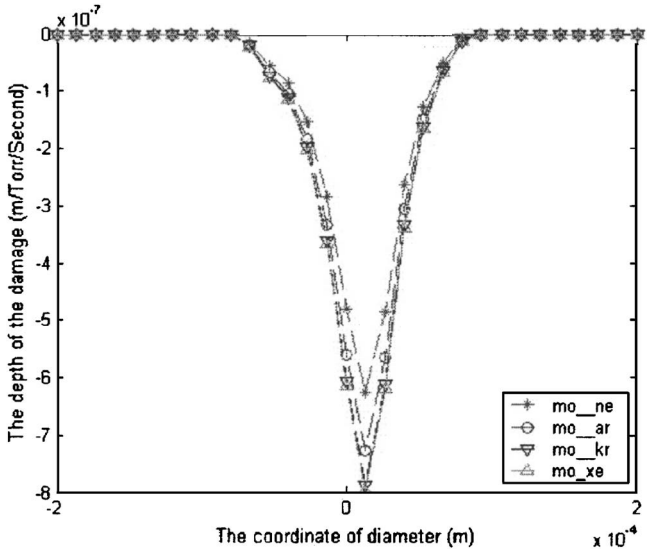

FIG. 8. Comparison of the ion bombardment damages induced by Ne, Ar, Kr, and Xe on a Mo-microtip cathode.

cathode, hop electrode and anode are 0, 400, and 1000 V, respectively. The number of electrons emitted from cathode is about 8000.

As mentioned earlier, the cathode damage caused by ion bombardment is determined by the cathode material, the residual gas type, and the electron beam current. In this article, we calculated ion bombardment damage of different cathodes due to different residual gas types.

Eight different situations have been investigated. The cathode and residual gas inputs are shown in Table I.

For each combination as shown in Table I, the potential distribution and the trajectories of the primary electrons and the secondary electrons were calculated first, followed by the calculation of the ion generation and their trajectories.

In Fig. 5(a) the electron trajectories are shown and Fig. 5(b) depicts the trajectories of the positive ions. As discussed earlier, the ionization happens both in the hop region and the acceleration region.

Figures 6(a) and 6(b) show the cathode damage induced by argon on a silicon and a molybdenum cathode. Because of using the Monte Carlo method in the simulation, the cathode damage is not completely symmetric. From the comparison, we can see that damage induced by Ar on Si is larger than the damage on Mo. For a specific type of residual gas, the damage on the target material is depending on the target's atomic mass M_t and its atomic number Z_t. The value of M_t, Z_t for silicon is 28.09 and 14, while the corresponding value for molybdenum is 95.94 and 42. From Fig. 6(c) as well as from the Eqs. (1)–(6) we see that the damage on Si is larger than the damage on Mo for the ionized Ar atoms.

Besides Ar, we also compared the damages induced by Ne, Kr, and Xe to silicon and molybdenum, and the results are similar to the result as showed in Fig. 6.

In Figs. 7 and 8 the damage induced by different residual gases to the same target are shown. From Fig. 7 we can see that the ion damage on the silicon target induced by Ar, Kr, and Xe is more destructive than induced by Ne on silicon. Figure 8 also shows that Ar, Kr, and Xe are more destructive than Ne to the molybdenum cathode. The damage on the same target depends on the type of projectile. The values of M_t, Z_t for Ne is 20.18 and 10, for Ar is 39.95 and 18, for Kr is 83.80 and 36, and for Xe is 131.3 and 54. Furthermore, the damage also has a relationship with the ionization energy of the residual gases. The value of the ionization energy of Ne, Ar, Kr, and Xe are 21.564, 15.759, 13.999, and 12.130 eV, respectively. So the lager the atomic number of residual gas, the easier it will be ionized. From the simulations, we conclude the following result: the larger the atomic number of residual gas, the more destructive damage it will induce.

IV. SUMMARY AND CONCLUSION

By calculating the process of electron emission, the trajectories of the electrons that travel through the hop and flu spacer and the ion generation, we obtained the ion bombardment on the cathode surface in the structure of a HOPFED type of display. In our simulation, the cathode material is silicon and molybdenum; the residual gas type is neon, argon, krypton, and xenon. And the ion bombardment damage on cathode is compared. From the comparison, we conclude that: The damage induced by Ne, Ar, Kr, and Xe on Si is larger than that on Mo. This is because the atomic mass M_t and atomic number Z_t of Si is smaller than that of Mo. Damage induced by different residual gases to the same target depends on the type of projectile. Ion damage on the silicon target induced by Ar, Kr, and Xe is more destructive than Ne to silicon, also ion damage on molybdenum induced by Ar, Kr, and Xe is more destructive than Ne to molybdenum. This is because of the different atomic mass, atomic number, and ionization energy of the residual gases. The simulation result indicates that the larger the atomic number of residual gas,

the more destruction it will induce. We also conclude that a molybdenum emitter is more stable than a silicon emitter in a nonideal vacuum environment.

ACKNOWLEDGMENTS

The work of this article is supported by the National Key Basic Research Program 973 (2003CB314706), the Foundation of Doctoral Program of Ministry of Education (20030286003), and the Foundation of Southeast University Science and Technology (XJ030611, XJ030612). The PPD department of LG.Philips Display Company provides the simulation tool. The authors express great thanks to them for this help.

[1]H. M. Visser *et al.*, Proc. of the SID'03 (2003), pp. 806–809.
[2]S. Tominetti and M. Amiotti, Proc. IEEE **90**, 4 (2002).
[3]X. Zhong *et al.*, Proceedings of ASID'04, pp. 203–206.
[4]G. G. P. van Gorkom *et al.*, Appl. Surf. Sci. **111**, 276 (1997).
[5]H. Seiler, J. Appl. Phys. **54**, R1 (1983).
[6]J. J. Scholts, D. Dijkkamp, and R. W. A. Schmitz, Philips J. Res. **50**, 375 (1996).
[7]G.-J. Zhang, W.-B. Zhao, and Z. Yan, Discharges and Electrical Insulation in Vacuum 622 (2002).
[8]Y. S. Choi, S. N. Cha, S. Y. Jung, J. W. Kim, J. E. Jung, and J. M. Kim, IEEE Trans. Electron Devices **47**, 1673 (2000).
[9]A. Shih, J. Yater, C. Hor, and R. Abrams, Appl. Surf. Sci. **111**, 251 (1997).
[10]O. Yamamoto, T. Hara, T. Takuma, H. Matsuura, Y. Tanabe, and T. Konishi, Discharges and Electrical Insulation in Vacuum, ISDEIV, XVIIth International Symposium on **1**, 502 (1996).
[11]T. Higuchi *et al.*, Appl. Surf. Sci. **200**, 125 (2002).
[12]R. H. Reuss and B. R. Chamala, Inf. Disp. **7**, 28 (2001).
[13]P. C. Zalm, J. Appl. Phys. **54**, 5 (1983).